Incoherent Scatter Radar Observations of Westward Electric Fields and Plasma Densities in the Auroral Ionosphere, 1

P. M. BANKS[1]

Radioscience Laboratory, Stanford University, Stanford, California 94305

C. L RINO AND V. B. WICKWAR

Stanford Research Institute, Menlo Park, California 94025

This paper reports the results of incoherent scatter radar observations of high-altitude ion drifts and other plasma parameters made February 24, 1972, at Chatanika, Alaska ($L = 5.7$), during a period of magnetic disturbance. For this experiment, conducted between 0909 to 1303 UT (2309 to 0303 AST), the radar line of sight was held fixed in the magnetic meridian plane so that the observed north-south ion drifts could be interpreted in terms of a westward electric field that ranged in magnitude from -10 to $+35$ mV m^{-1}. The results confirm many effects found previously through other experimental techniques. Southward ion drifts predominated during the 4-hour observation period. Several times the westward electric field inside large regions of enhanced electron density was substantially smaller than the field outside these regions. In addition, on several occasions these walls or bands of ionization were found to drift southward at about the same speed as the $\mathbf{E}_\perp \times \mathbf{B}$ drift in the surrounding plasma. The plasma inside the enhanced region, however, did not share the drift motion but remained relatively stationary with respect to the radar. The present observations of F_2 layer densities and temperatures indicate an unusual increase in electron density just before the onset of a large substorm. Finally, measurements of the height and peak density of the auroral E layer show significant variations in the intensity and average energy of the electron flux. These variations appear to be related to auroral breakup and a transition to steady precipitation of moderately soft electrons.

Measurements of electric fields in the auroral ionosphere have been made by a variety of methods. These include: (1) direct measurements by rocket probes [e.g., *Mozer and Bruston*, 1967; *Aggson*, 1969; *Potter and Cahill*, 1969; *Mozer and Fahleson*, 1970; *Potter*, 1970; *Fahleson et al.*, 1971; *Kelley et al.*, 1971*a*; *Choy et al.*, 1971; *Bering et al.*, 1973], satellite probes [*Cauffman and Gurnett*, 1971; *Heppner*, 1972], and balloon-borne double probes [*Mozer and Serlin*, 1969; *Mozer and Manka*, 1971; *Kelley et al.*, 1971*b*; *Mozer et al.*, 1973], and (2) indirect measurements through observations of the motions of ionized barium clouds [e.g., *Föppl et al.*, 1968; *Wescott et al.*, 1969, 1970; *Haerendel et al.*, 1969; *Haerendel and Lüst*, 1970; *Fahleson et al.*, 1971; *Heppner et al.*, 1971; *Haerendel*, 1972, unpublished manuscript, 1973], by incoherent scatter radar [*Doupnik et al.*, 1972; *Banks et al.*, 1973, manuscript in preparation, 1973], and by satellite-borne ion current probes [*Galperin and Ponomarev*, 1972], and (3) observation of drift motions of visible aurora [*Davis*, 1971; *Kelley et al.*, 1971*b*; *Subbarao and Rostoker*, 1973].

In two previous studies [*Doupnik et al.*, 1972; *Banks et al.*, 1973] and in a third study whose results are being prepared for publication (Banks et al., 1973) the incoherent scatter radar at Chatanika, Alaska ($L = 5.7$, $\Lambda = 65.2°$), has been used to infer electric fields from ion Doppler shifts in the ionosphere at altitudes greater than 150 km where the relation $\mathbf{v}_\perp = \mathbf{E}_\perp \times \mathbf{B}/B^2$ is valid. Owing to the intrinsic limitations of a monostatic radar site, the ion Doppler velocities needed to determine $\mathbf{v}_\perp$ and $\mathbf{E}_\perp$ are obtained by consecutive measurements in three separate directions. As a consequence, large-scale temporal and spatial filtering effects are introduced into the radar data. With regard to the temporal resolution, the pattern of consecutive measurements permits new ion velocity vectors to be constructed every 10 min, but the overall time required for truly independent velocity vectors is about 30 min. In addition, the individual line of sight ion velocities are obtained from points separated by about 107 km at 170-km altitude. Although such smearing is acceptable for many purposes dealing with the gross behavior of diurnal electric fields and ionospheric E region current densities, a finer resolution is essential for investigating electric fields associated with substorms and auroras.

Attempts to improve the space-time resolution of electric field measurements have been made in a recent series of magnetic meridian experiments at Chatanika. By keeping the radar antenna fixed in the magnetic meridian plane at an elevation angle of 45°, the north-south drift speed of ions can be determined at 1-min intervals in range gates that have an effective length of about 45 km. In addition, the electron density can be simultaneously measured along the radar line of sight in 192 overlapping range gates of 10-km width.

Additional meridian plane measurements were made in February and March 1973 and will be reported in a later paper [*Rino et al.*, 1973]. In the present paper, results are given for a similar experiment conducted inadvertently (owing to low temperatures, the radar antenna was kept stationary in the magnetic meridian plane) in the evening hours of February 24, 1972. This period was characterized by a high level of magnetic activity, and the experimental results illustrate a number of important features of auroral

[1] On leave of absence from the University of California at San Diego, La Jolla, California 92037.

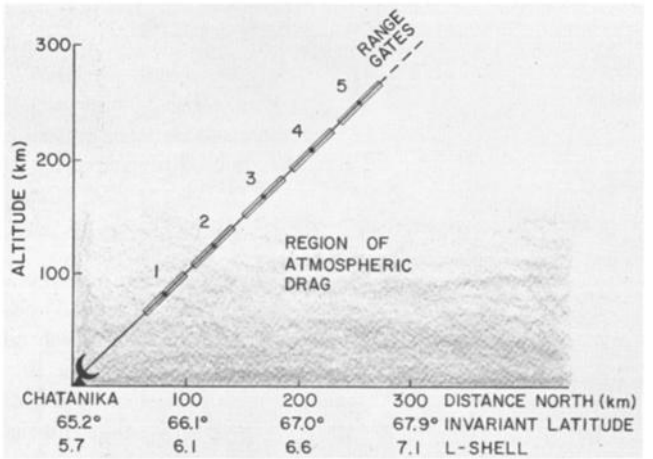

Fig. 1. Schematic view of Chatanika spectral range gates for the experiment of February 24, 1972, in the period 1000–1300 UT. Ion velocities from range gate 3 (167-km altitude) provided the data needed to compute E-W electric fields.

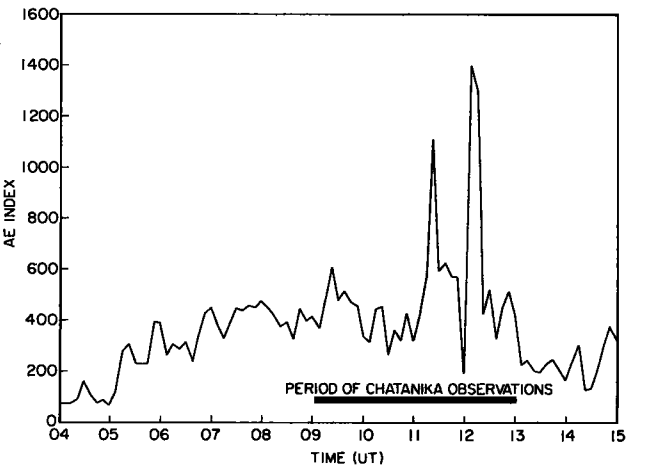

Fig. 3. Auroral electrojet index (AE) for February 24, 1972. Data were provided by the NOAA World Data Center.

electric fields and auroral motions. Though we cannot generalize the present results to all conditions, the study provides a unique view of various interrelated auroral phenomena.

The principal results of this study, to be discussed in the following sections, include the following.

1. During the 4 hours of the experiment, southward ion drifts were predominant.

2. There were several times when the westward component of the electric field was small inside extended bands or patches (up to 50 km wide) of high electron density.

3. These regions of high electron density drifted southward at about the same speed as the $\mathbf{E}_\perp \times \mathbf{B}$ drift seen in adjacent regions of relatively low electron density.

4. The southward drift of the ionization enhancements was most strongly evident during the recovery phase of a local midnight sector substorm. However, southward drifts of enhanced ionization regions were also seen several times in the hour before the substorm.

5. The largest drifting ionization enhancement could be identified with visible auroral emissions.

6. A very intense F_2 layer appeared 30 min before a substorm with a southward drift of 400m sec^{-1}, then vanished within 1 min after substorm onset. Coincident with the removal of the F_2 layer ionization, an enhanced auroral E layer appeared.

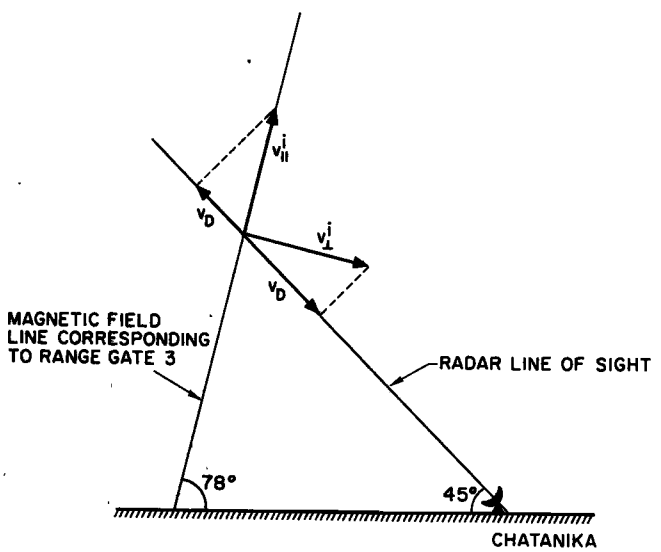

Fig. 2. Measurements of N-S ion velocities reflect ion motions parallel and perpendicular to **B**. Since F region velocities parallel to **B** are usually much smaller than the perpendicular velocities, the present experiment measures principally $v_\perp^i$.

DESCRIPTION OF EXPERIMENT

The incoherent scatter radar system at Chatanika, Alaska, has been described by *Leadabrand et al.* [1972] and *Baron* [1972], while the basic principles of the incoherent scatter method have been reviewed by *Evans* [1969, 1972]. The radar operates in a monostatic mode at 1290 MHz using two interspersed pulse lengths. A long pulse, lasting 320 μsec, is used to determine ion Doppler shift and electron and ion temperatures in eight range gates of about 45 km effective length which are separated by a distance of 60 km. (Details of the data processing procedures are given by *Baron et al.* [1970] and *Rino* [1972], while the results of other experiments using the radar have been reported by *Doupnik et al.* [1972], *Bates et al.* [1973], *Watt* [1973], *Brekke et al.* [1973], and *Banks et al.* [1973].) In addition to the long-pulse spectral channel, a short 67-μsec pulse is used to provide electron density data from 192 overlapping range gates having effective widths of 10 km. For both

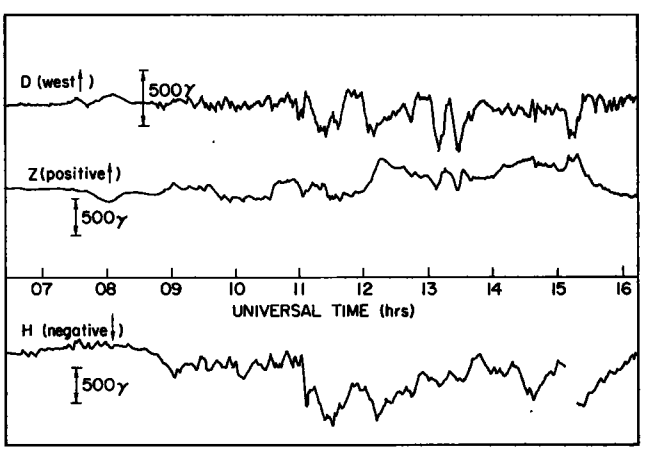

Fig. 4. College magnetogram for February 24, 1972.

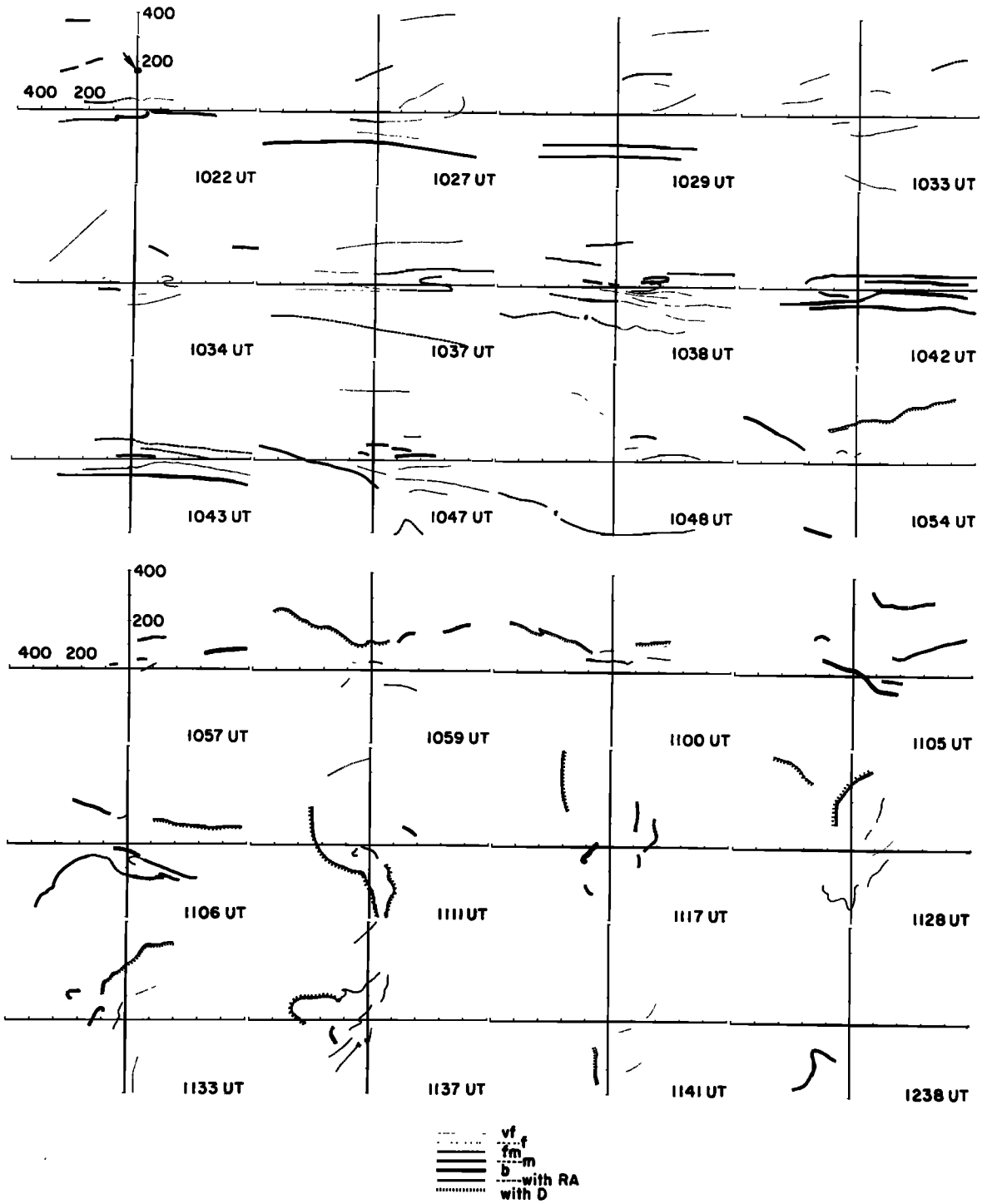

Fig. 5. Auroral maps obtained from 35-mm Chatanika all-sky camera photographs. Directions are geomagnetic, north being at the top, east to the right. The arrow and dot at 1022 UT indicate the center of the radar third range gate. Distances are given in kilometers. Legend: vf, very faint; f, faint; fm, faint to medium; m, medium; b, bright; RA, with rayed arcs; D, with diffuse arcs.

spectral and density channels the antenna beamwidth gives a probing diameter of 2.1 km at 200 km range.

It is difficult to calculate the statistical uncertainty of the radar Doppler shift measurements, but various tests made with injected radio signals of known frequency shift indicate a rms error of ± 20 msec^{-1} for a signal to noise ratio greater than about 0.3 and 1-min integration. For this relatively short signal integration period, which is used here (1 min), and the typically low plasma densities in the present experiment, signal to noise ratios lower than 0.3 were occasionally encountered, and the velocity resolution with 1-min integration was clearly degraded. Examination of the results, however, indicates that the resolution was probably no worse than ± 50 msec^{-1} or an equivalent perpendicular electric field of ± 2.5 mV m^{-1}.

The present experiment started at 0909 UT, February 24, 1972, and ended at 1303 UT (local time = UT − 9 hours 51 min; corrected geomagnetic time = UT − 11 hours 10 min). During the experiment the antenna azimuth was kept at 0° magnetic so that only the north-south compo-

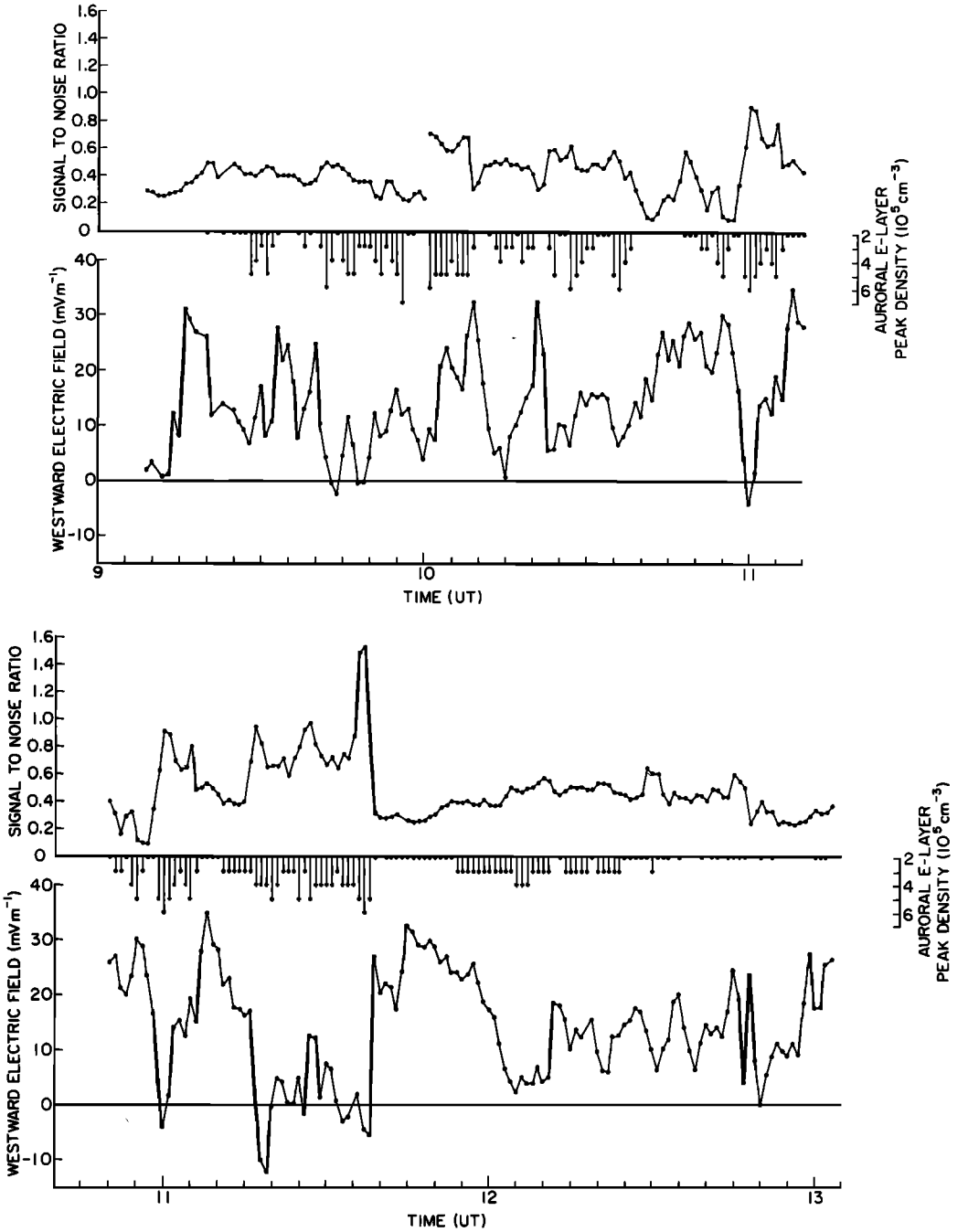

Fig. 6. Values of the westward component of the ionospheric electric field perpendicular to **B** obtained with 1-min data averages for (*top*) 0907–1110 UT and (*bottom*) 1020–1310 UT. The range gate 3 signal to noise ratio is proportional to the spectral channel electron density. The peak density of the auroral *E* layer is also shown.

nent of ion motions could be observed. For the first hour (0909 UT to 1000 UT) the antenna elevation angle was 60° above the horizon. At 1000 UT the elevation angle was changed to 45° and was kept there for the rest of the experiment. The geometry for the latter part of the experiment is shown in Figure 1.

From previous work [*Doupnik et al.*, 1972; *Brekke et al.*, 1973] it has been found that the effect of atmospheric drag is important below about 150 km and that the lowest two spectral range gates illustrated in Figure 1 cannot be used to infer ionospheric electric fields. To verify the lack of atmospheric drag, ion velocity data from the range gates at 167 and 209 km have been compared and found to agree very closely.

It also follows from Figure 1 that the measured ion Doppler shifts can arise from ion motions parallel and perpendicular to the magnetic field **B** (see Figure 2). For the present geometrical arrangement an ion motion of 100 m sec^{-1} parallel to **B** (and outward) would give a line of sight velocity of 54.5 m sec^{-1} away from the radar, whereas a southward ion motion of 100 m sec^{-1} perpendicular to **B** and in the plane of observation would give a line of sight velocity of 83.8 m sec^{-1} toward the radar. Previous Chatanika measurements of ion motions in the *F* region have shown that ion velocities parallel to **B** as large as 100 m sec^{-1} are not common, typical values being on the order of 50 m sec^{-1} or less even during high levels of substorm activity [*Baron*, 1972]. Since the peak *F* region north-south velocities measured in this experiment were of

the order of 300 to 600 m sec^{-1}, we have assumed that the observed ion spectrum Doppler shifts in range gate 3 (167-km altitude) correspond to ion drift under the action of an E-W component of the perpendicular electric field whose magnitude follows from the relation $\mathbf{E}_\perp = -\mathbf{v}_\perp \times \mathbf{B}$.

Before the experimental results are presented, two additional details must be discussed. The first is the effective spatial resolution of the spectral channel range gates. As *Rino* [1972] and *Brekke et al.* [1973] pointed out, the spectral data are processed through autocorrelation techniques, so that a given velocity estimate encompasses data from a 96-km range spread. However, the measured ion velocity is an average value that involves an effective triangular weighting function, an R^{-2} range dependence, and the range profiles of electron density and ion Doppler shift. These quantities are spatially integrated along the radar line of sight to give the observed Doppler shift in a given range gate. As a consequence, the width and peak response range of a given gate can vary slightly with changes in the range distribution of electron density and ion velocity. For typical E and F region conditions, however, it seems that the effective widths of the spectral gates are about 45 km (J. R. Doupnik, personal communication, 1973).

The second detail is the short-pulse measurements of electron density. The total power received is proportional to the electron density modified by a range R^{-2} factor and a plasma temperature factor:

$$n_e/n_e' \cong (1 + \alpha^2)(1 + r + \alpha^2)/2$$

where $r = T_e/T_i$ and α^2 is the Debye length correction, $\cong 14T_e/n_e$ [*Evans*, 1969].

Owing to the expense of computation, the electron densities given here do not include the temperature correction factors. As a consequence, the electron densities above about 200 km are underestimates such that at 300 km the results could be too small by 50% if $r = 2$. However, this underestimate at high altitudes does not affect the present analysis in any direct way. Further details of the normalization of the electron density data are given by *Baron* [1972].

Background Geophysical Conditions

This experiment was conducted during a period of highly disturbed magnetic and auroral conditions. The auroral electrojet index, shown in Figure 3, indicates that this activity commenced about 0500 UT and reached a peak in the period 1100 to 1230 UT. For reference, the magnetogram obtained at College, Alaska (located 27 km south of Chatanika), is shown in Figure 4. From these data it is clear that the large midnight sector substorm near College at 1100 UT was not isolated but occurred during a period of sustained magnetic activity that began in the College area at about 0840 UT.

Visible aurora were recorded during a portion of this experiment using a 35-mm all-sky camera (ASC) at Chatanika and 16-mm cameras at Ester Dome and Fort Yukon. Owing to excess light from the moon, the 16-mm photographs provided very little useful auroral information. Consequently, only the Chatanika ASC results are shown here. Rather than reproducing the ASC photographs directly, these data have been reduced to the auroral maps shown in Figure 5, for which an emission height of 110 km has been assumed. From these auroral maps it is apparent that the third range gate was substantially to the north of

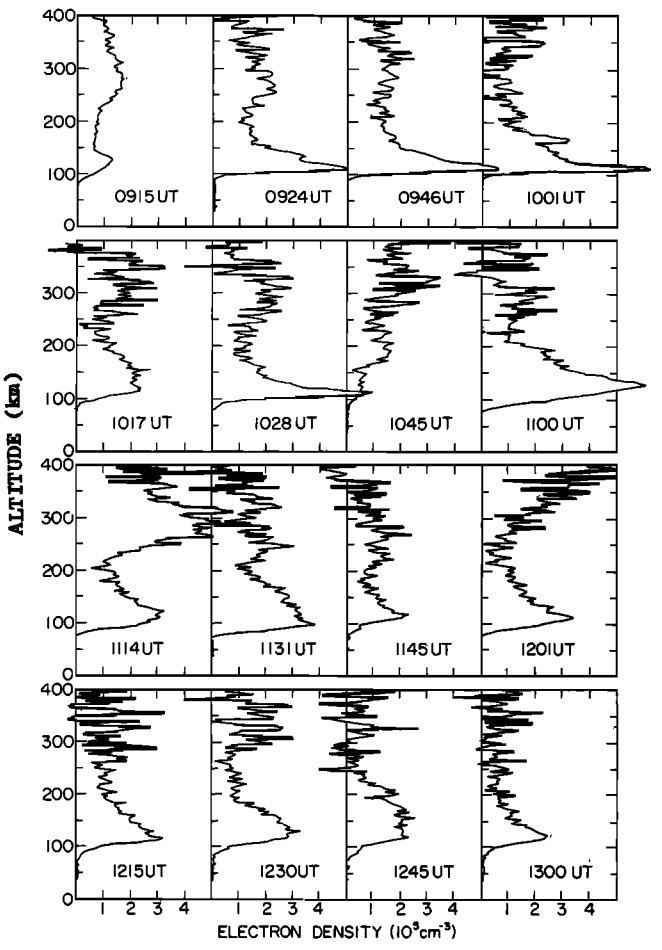

Fig. 7. Selected 1-min average electron density profiles as a function of altitude.

most visible auroral activity. Consequently, the observed electric fields can probably be characterized as those belonging to the poleward side of the auroral oval or perhaps even the outer edge of the polar cap.

A plot of the westward electric field component (E_w) inferred from 1-min averages of the third range gate ion velocity is shown in Figure 6. At the top of this figure are also shown the 1-min average signal to noise ratio (SNR) estimates for the third range gate. Since the SNR is proportional to electron density averaged over the entire spectral range gate, it provides a convenient reference to the spectral channel average electron density as a function of time.

Figure 6 shows that the east-west electric field component was almost completely westward during the entire observational period, the values ranging between -10 and $+35$ mV m^{-1}. Although there is some randomness to consecutive data points, the 1-min data averaging period appears to have been sufficiently short to resolve many short-term fluctuations of the electric field. There does not seem to be any unique feature in E_w before the 1100 UT substorm but, as Figure 3 shows, the series of disturbances began as early as 0840 UT, and the enhanced values of E_w reflect a high degree of activity for the College area.

In Figure 7 short pulse electron density profiles are shown for different times during this experiment. Auroral E and F layers are clearly evident but, owing to spatial effects, it is not possible to consider these data as giving

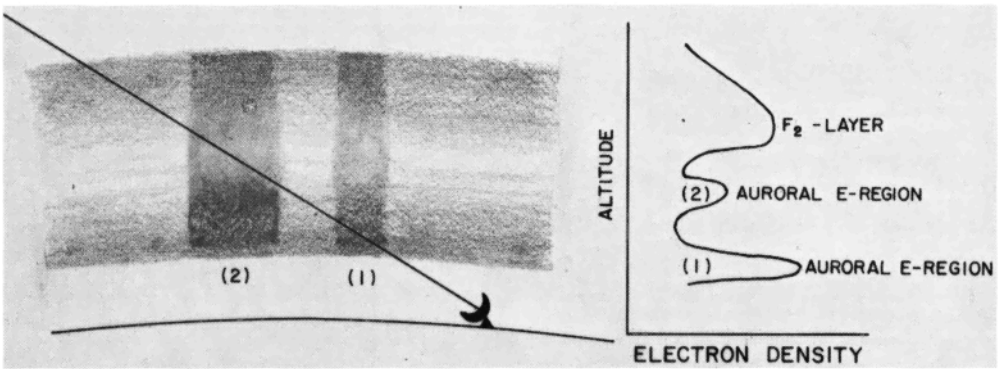

Fig. 8. Schematic diagram of the electron density range profile obtained in a spatially inhomogeneous ionosphere. The furthest density enhancement is intended to be the most intense, but owing to the way auroral ionization is distributed with altitude it appears less dense than the smaller enhancement seen in the E region.

true altitude profiles, since horizontal variations are frequently important. The profile obtained at 1001 UT, for example, shows not only an auroral E layer at 110 km, but also a higher-altitude slice of an auroral feature 165 km north of Chatanika. To demonstrate this effect, a schematic diagram of the profile that results when several separate regions of enhanced auroral ionization are present is given in Figure 8.

RESULTS

Anticorrelation of the westward electric field component and the electron density. Comparison of the results for E_w and the third range gate (167 km) SNR (see Figure 6) shows that there is often a tendency for an inverse correlation. Clear examples of this are seen at 1009, 1021, 1055, and 1248 UT and especially in the period after 1137 UT, when a large decrease in SNR was accompanied by a substantial increase in E_w. Likewise, periods of enhanced SNR (or electron density) were associated with significantly smaller values for E_w, the most notable occurrences being found near 1100 UT and 1115–1137 UT. At other times the trend toward an inverse relationship seems to be present in competition with other processes. The rise in E_w between 1100 and 1115 UT, for example, occurs during a time when the SNR is lower than during the preceding period of time, but whereas E_w reaches about the same magnitude as was seen at 1050 UT, the SNR is several times greater.

The connection between electric fields and electron density involves currents in the E region. *Mozer et al.* [1973], for example, have found that E_w is greatly reduced above regions where the electrical conductivity is enhanced by auroral precipitation. One difficulty in studying the relationship between electric fields and electrical conductivity variations in the present experiment lies in the need to determine the E region electron densities in the regions lying immediately below the third range gate. Anticorrelations between E_w and the third range gate SNR need not always occur, however, since an enhanced auroral E layer will not necessarily be seen as a proportionate enhancement in the electron density at 167 km.

An alternative way of investigating E region effects upon E_w involves the short-pulse observations of the auroral E layer. Although the portion of the auroral E layer sampled by the short-pulse method is about 50 km south of the region of the ionosphere sampled by the third range gate (see Figure 1 and the typical short-pulse range profiles in Figure 7), the rapid southward drift of the ionization sources observed during this experiment (discussed in the next section) implies that these lower-altitude densities may at times be useful to investigate the inverse electric field to electron density relationship. To show this, scalings of the peak E region densities from the short-pulse data have been included in Figure 6. As can be seen, there are a number of specific cases (1009, 1021, 1055, 1137, 1248 UT) when the inverse relationship seems to be present, especially when a 2-min delay time is introduced in the auroral E layer data to account for the southward drift of the ionization source.

It must also be pointed out, however, that E_w and the E region electron density may not be strictly anticorrelated. Though a number of measurements [*Aggson*, 1969; *Heppner et al.*, 1971; *Potter and Cahill*, 1969; *Wescott et al.*, 1970; *Potter*, 1970] indicate a marked tendency for $\mathbf{E}_\perp$ to be lower in the vicinity of aurora, other observations [*Mozer and Bruston*, 1967; *Kelley et al.*, 1971*a*, *b*; and *Choy et al.*, 1971] show no anticorrelation. More recent comparisons between $\mathbf{E}_\perp$ and auroral X ray and optical emissions have been made by *Mozer et al.* [1973]. These authors find a strong anticorrelation between E_w and electron precipitation; i.e., the result suggested by the present data. From their experiments

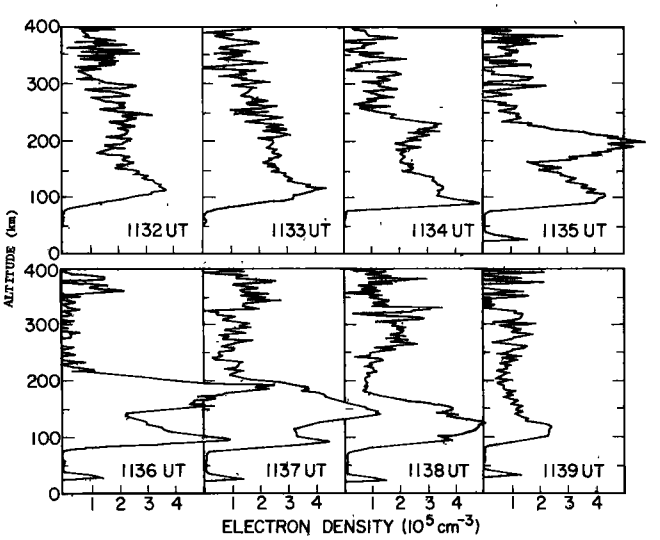

Fig. 9. Electron density profiles obtained for the period 1133 to 1138 UT showing the southward movement of a dense, thick wall of ionization. As the wall passes through the 115-km height (or horizontal range) there is no large enhancement of the E layer.

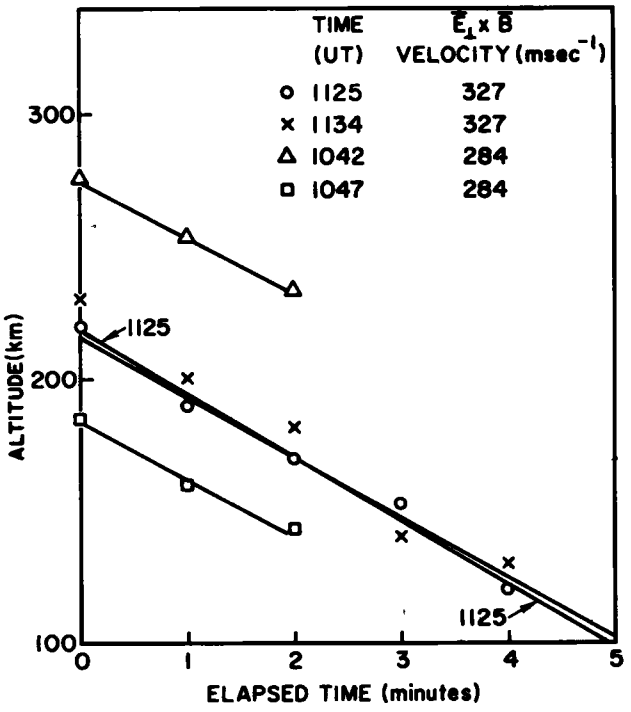

Fig. 10. Apparent altitude of electron density enhancements as a function of elapsed time.

decreases in E_w were found during precipitation events about 70% of the time.

Motions of auroral ionization enhancements. Analysis of the short-pulse electron density data shows that large bands (up to 50 km wide and 100 km high) of enhanced electron density had apparent southward drift speeds that were about the same as the average plasma speed outside the enhanced density regions. From the discussion of the last section, however, the velocity of the plasma inside the moving density enhancements was usually substantially smaller than that outside.

The best example of this behavior is found in the period 1134 to 1138 UT, when an extended region of enhanced electron density appeared to move southward toward Chatanika. This motion is shown in Figure 9, where density profiles are shown for several consecutive data integration periods. This ionization enhancement was first seen at an apparent height of 225 km. As time passed the high-density region appeared to move toward Chatanika, vanishing from view after 1138 UT. The southward component of drift velocity (perpendicular to **B**) was 327 m sec^{-1} as determined by a least squares fit to the apparent altitude of the peak as a function of time (see Figure 10). This velocity corresponds to an equivalent electric field of 17 mV m^{-1}, i.e., close to the 20 to 25 mV m^{-1} electric field seen immediately before and after the enhanced density region passed through the third range gate. During the time this region was within the third range gate, the inferred westward electric field was very small, indicating that, while the region itself was drifting, the plasma inside the enhanced region was not moving appreciably. A schematic diagram of this peculiar situation is given in Figure 11. In principle this behavior appears to agree with the recent model of *Kelley et al.* [1971*b*], where ionization sources are thought to undergo $\mathbf{E}_\perp \times \mathbf{B}$ drifts even though E_w inside the region of enhanced density remains small.

Another important aspect of the 1134–1138 UT ionization region is seen in the abrupt increase in E_w at the time that the third range gate SNR decreased (1138 UT) after the ionization region had passed. Through examination of the ion velocity data from range gates 4 through 7, shown in Figure 12(*a*), it can be seen that the change of E_w appeared to propagate southward toward Chatanika at a speed of 495 m sec^{-1} (see Figure 12*b*). In this case it seems that the region of enhanced E_w moved in conjunction with a boundary of greatly reduced precipitation and low E region electron densities. This observation supports the idea of anticorrelation between E_w and region conductivity. This abrupt transition and its implications are further discussed in the next section.

Finally, we must note that the ionization structure seen between 1134 and 1138 UT has been described in terms of a patch or band. Actually, the term 'ionization wall' would be more appropriate, since it is clear from Figure 9 that the density enhancement was at least 50 km wide and had an altitude extent of at least 100 km; i.e., from the lower F_2 region down to the E region. It is within the horizontal confines of this wall that E_w was substantially reduced in comparison with the external electric field. As is shown by the data of Figure 9, the wall itself underwent a rapid southward drift.

The detection of drifting ionization regions was not confined to postsubstorm (1100 UT) times. Such motions could be identified during virtually every 10-min period between

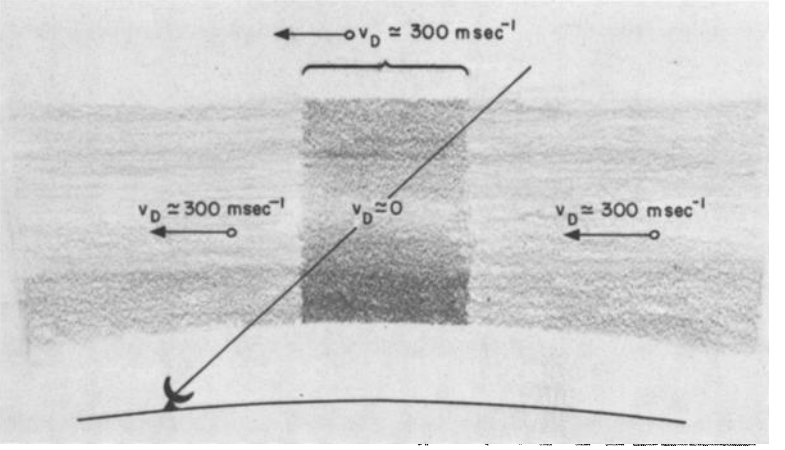

Fig. 11. Schematic illustration of the observed plasma drift velocities in the vicinity of a large density enhancement.

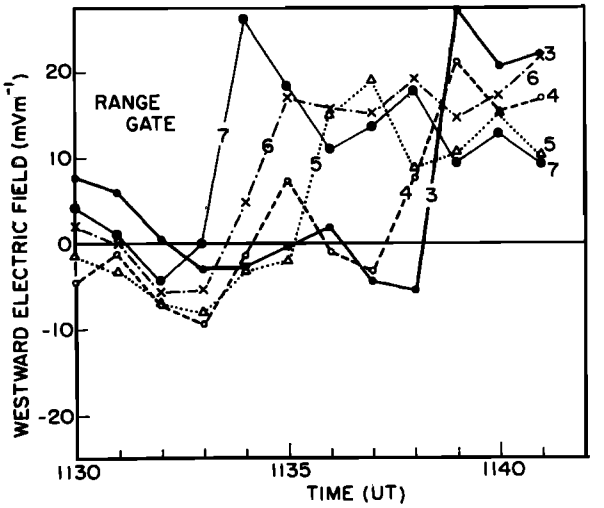

Fig. 12a. Westward electric fields obtained from range gates 3 through 7 as a function of time.

1000 and 1300 UT. Three additional examples of such drifts, included in Figure 10, show speeds of 284 and 337 m sec^{-1}. However, the corresponding condition of there being a smaller electric field within the enhanced ionization region could be definitely made only for ionization enhancements seen at 1015, 1100, 1117, and 1134–1137 UT.

Drifting regions of high ionization density and associated electrical currents are also found in the College magnetic records. As is shown in Figure 13, from 1050 to 1150 UT variations of E_w were matched by similar amplitude variations in the magnetic H and D components. However, a time lag of about 5.5 min can be seen between the two quantities. Such a period corresponds to the time required for an ionization region to travel from the third range gate to the vicinity of College at a speed of about 350 m sec^{-1}. This strongly implies that the structure of the westward electric field component between 1050 and 1150 UT was determined by the spatial distribution of the ionospheric electron densities moving past the third range gate and the College magnetic observatory.

The electron density enhancement seen between 1134 and 1138 UT had an apparent southward speed of 327 m sec^{-1}.

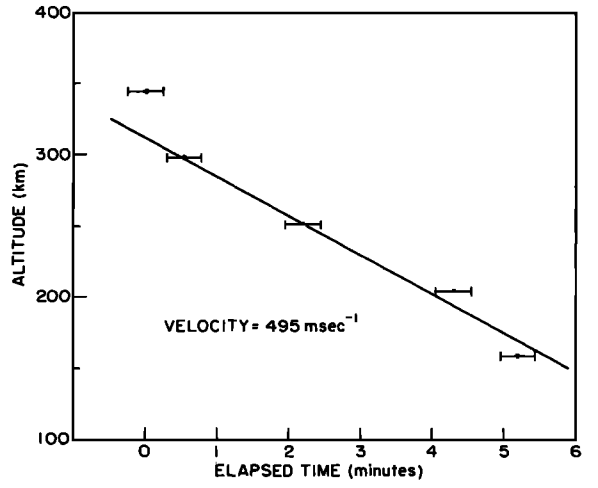

Fig. 12b. Altitude (or horizontal range) of the zero crossings of Figures 12a as a function of time. The solid curve gives the least squares fit to the data. The error bars correspond to the 1-min averaging times.

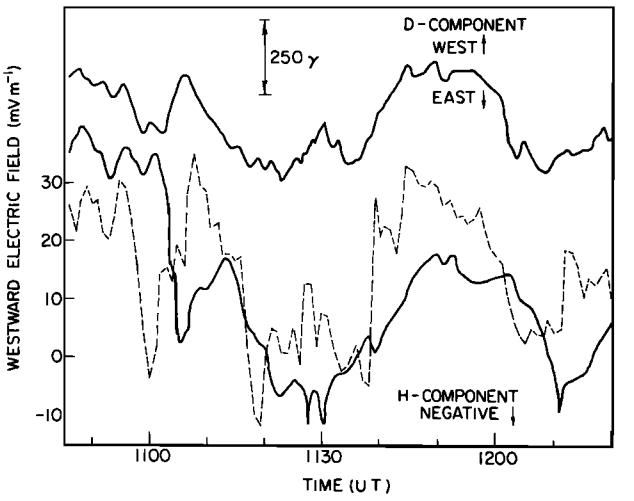

Fig. 13. Comparison of the westward electric field deduced from range gate 3 (dotted curve) and the College H and D components of the magnetic field (solid curves). The time delay of 5.5 min near 1100 UT between E_w and H (and D) corresponds to a 350 m sec^{-1} southward motion for the region of electrical current flow.

Examination of the ASC records indicates that this enhancement corresponded to a diffuse rayed band seen at 1133 UT and 1137 UT moving southward with an average speed of about 300 m sec^{-1}. Owing to its faintness (which is a consequence of its motion), the width of this band cannot be determined from the ASC records. The radar, however, indicates precipitation over a 50-km-wide region. Enhancements seen earlier in the experiment cannot be readily identified with specific auroral forms. Examination of the ASC records in the period after 1100 UT, however, indicates a generally southeasterly motion of visible forms with speeds between 300 and 500 m sec^{-1}. After 1138 UT it was difficult to find any auroral emissions in the ASC records. Photometer observations of 6300 A emissions in a 5° cone at the Chatanika zenith show clearly the passage of a 5-kR or greater emission feature associated with the 1133–1137 UT diffuse rayed band. The time of appearance of this emission feature was in good agreement with the radar-observed drift speed of the E region density enhancement.

Before passing to the next topic, we note that the motion of auroral ionization creates a special observational problem for the analysis of the radar data. To obtain respectable electron density range profiles, it is necessary to time-average the scattered radar signal. However, a moving ionization band will remain in a particular range gate only for a short time. At 400 m sec^{-1}, for example, a narrow ionization band passes through a 10 km wide gate in 25 sec. Thus, though one would like to integrate the electron density data only over the time it takes the ionization band to pass through the range gate, the statistical nature of the radar signal requires longer times to obtain good signal-to-noise ratios for the background plasma in adjacent ranges.

Electron densities. A substantial auroral E layer was present during most of this experiment. The density variation of this peak has been shown in Figure 6 and is repeated in Figure 14 in conjunction with the observed variation of the apparent height of the maximum electron density. The uncertainty surrounding the true height of the peak density is unfortunate, but by looking at general trends and remembering that there is considerable evidence for south-

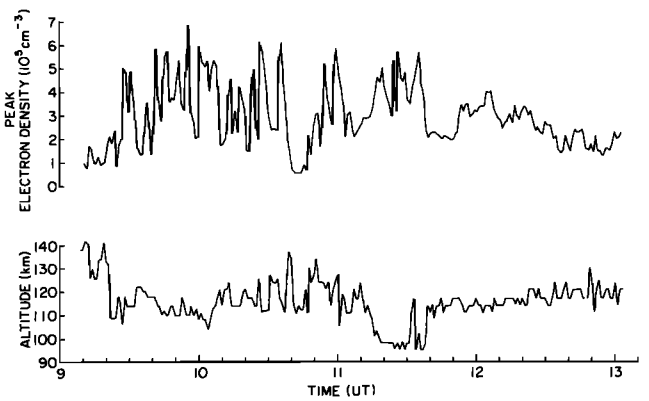

Fig. 14. The measured variation in the peak auroral E layer electron density is shown as a function of time in the upper plot. The apparent height of the layer is shown below.

ward motion of the ionization regions, we can get some average notion about changes in the height of the E layer.

During the first 2½ hours of the experiment the auroral E layer was highly structured as new forms continually appeared or intensified in the radar line of sight. A pronounced minimum in electron density near 1038 UT was followed by a gradual increase marked by substantial variations. From ASC records (see Figure 5), there was a sharp brightening of auroral forms first seen at 1042 UT which could have signaled the onset of a substorm. However, there is no evidence for subsequent expansion and breakup phases, and so this brightening cannot be regarded as more than a period of enhanced magnetospheric activity.

Comparison of Figures 14 and 4 shows that the intense negative bay observed at 1100 at College was not associated with any special intensification of the particle flux or hardening of the energy spectrum at the radar E layer penetration region 110 km north of College. In fact, the only unusual change seemed to center in the period 1110 to 1138 UT when, as deduced from the decreased altitude of the auroral E layer, the energy of the precipitating electrons increased greatly. Use of the electron flux/energy nomographs given by *Chesnut et al.* [1971] suggests that the electron densities observed at this time could have been produced by an electron flux of $\sim 5 \times 10^7$ electrons cm^{-2} sec^{-1} ster^{-1} having a mean energy of ~25 keV. The auroral forms detected by the ASC and shown in Figure 5 suggest that the transition to a hard electron flux was associated with auroral breakup and the passage of a westward surge through the radar line of sight.

After 1138 UT there was a marked change in the character of the E layer, with an abrupt transition to rather steady precipitation typical of 6-keV electrons with a flux of $\sim 10^8$ electrons cm^{-2} sec^{-1} ster^{-1}. As was discussed earlier, it was at this same time that E_w showed what appears to be a related abrupt increase.

Another interesting feature of the present data is the behavior of the F_2 region near the time of the 1100 UT negative bay. In Figure 15 profiles of 1 min averaged electron density show the growth of an abnormally large F_2 layer to the north of Chatanika in the period before 1100 UT. The observed densities are substantially larger than those normally observed by the radar [e.g., *Watt*, 1973; *Bates et al.*, 1973]. From range gate 5 ion velocity data, this intense F_2 layer was moving southward at a velocity of 400 m sec^{-1}. Unlike the walls of enhanced ionization seen at lower altitudes, this region of enhanced density did not extend appreciably downward; i.e., the observed density was part of a moving layer rather than the upper part of an ionization anomaly.

Following the initial development of this enhanced F_2 layer, one finds that the ionization density remained rather steady until 1100 UT, when the F_2 region ionization dropped to very low values within 1 min. During the next 15 min the F_2 region recovered to some extent, perhaps in conjunction with the passage of the westward surge that followed the 1100 UT substorm. The growth of this unusual F_2 layer coincided with the 1042 UT brightening of auroral arcs (see Figure 5) and the general increase in the intensity of the auroral precipitation before 1100 UT.

At the present time it is necessary to regard the sudden appearance of a dense F_2 layer just before the 1100 UT substorm onset as a coincidence. This behavior was not repeated during the February and March 1973 experiments (which are not reported here). However, the presence of anomalously large F_2 regions that frequently appeared and disappeared was noted during the large August 4–9, 1972, magnetic storm (M. Baron, personal communication, 1973).

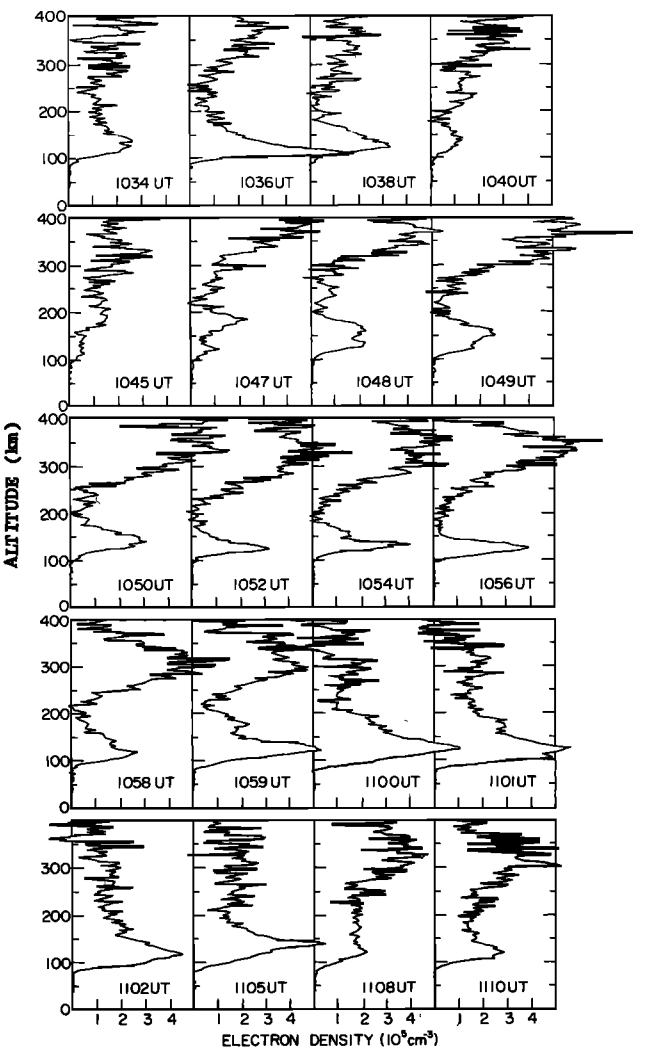

Fig. 15. Profiles of ionospheric density as a function of apparent altitude in the period 1034 to 1110 UT. The gradual growth of a dense F_2 region followed by its disappearance at 1100 UT is unusual. During this period the F_2 layer had a southward velocity of about 400 m sec^{-1}.

Finally, although there is some slight indication that the equatorward edge of the dense F_2 layer was seen to propagate toward Chatanika (see Figures 7 and 15), it is not possible to identify particular southward-moving features such as was possible for the E and F_1 region using range gate 3 and the short-pulse measurements of electron density.

Thermal structure. During this experiment measurements of electron and ion temperatures were obtained at F region heights. The results, shown in Figure 16, were obtained with 10-min integration periods using techniques described by *Baron* [1972].

With regard to the electron temperature, the most striking feature occurred in the period 1040 to 1100 UT, when T_e was 1400°K lower than temperatures measured before and after this time. This abrupt decrease appears to be closely linked with the previously described dense F_2 layer that moved into sight of the furthest radar range gates near 1040 UT. Since the electron to ion energy transfer rate is proportional to n_e^2, the high values of n_e in the enhanced F_2 layer should, as observed, lead to a substantial reduction in T_e.

The present values of T_e at 300 km tend to be substantially higher (500°–1000°K) than those recently reported by *Bering et al.* [1973] from a Langmuir probe rocket measurement. However, the extensive incoherent scatter radar measurements of temperatures and electron densities described by *Watt* [1973] indicate a wide variability in T_e during periods of auroral activity. Thus there is no particular significance to the difference between rocket and radar observations.

Two ion temperature curves are shown in Figure 16 corresponding to 211 and 300 km altitude. No features similar to those seen for T_e are present, but there is a marked tendency for T_i to increase up through 1130 UT to values near 1600°K at 300 km altitude. Normally, values of T_i at 300 km reflect the neutral gas temperature. However, owing to the effects of Joule heating associated with large relative bulk flow velocities between the ions and neutral gas, this condition is probably not true in the present case.

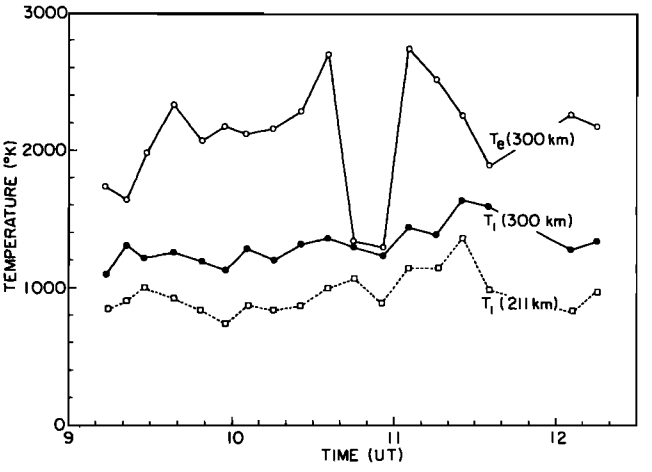

Fig. 16. Measured values of electron and ion temperature during the experiment. The large dip in T_e at 300 km is a consequence of the large F_2 layer shown in Figure 15.

DISCUSSION

The results of this experiment provide both confirmation for a number of processes previously detected in the auroral ionosphere and evidence for several new features.

The relationship between westward electric fields and the motion of auroras has been studied by *Kelley et al.* [1971*b*], *Davis* [1971], and *Subbarao and Rostoker* [1973]. In agreement with these earlier measurements, this experiment shows that the southward motion of auroral ionization enhancements can, within the accuracy of the present technique, take place at the $\mathbf{E}_\perp \times \mathbf{B}$ drift velocity. In one specific instance (1134 to 1138 UT), it was also observed that the plasma within the moving region of enhanced density was virtually stationary with respect to the radar. The observation that drifting density enhancements are connected with lower values of E_w agrees with the discussion of *Kelley et al.* [1971*b*] and *Mozer et al.* [1973] and indicates that, at times, the magnetospheric source of auroral electrons may move under the action of an $\mathbf{E}_\perp \times \mathbf{B}$ drift even though the ionospheric E_w is rather small.

The most striking anticorrelation of electron density and E_w occurred at 1138 UT when abrupt sequential increases in ion velocity were seen in the five spectral range gates beginning at the furthest range (see Figure 12*a*). During this same period, ASC and E region density data show that there was a transition from intense, rapidly fluctuating precipitation to a much smoother, uniform behavior. From the last section, our interpretation of this period is that the rise in E_w corresponded to the southward passage of a precipitation boundary that eventually left Chatanika in a region of relatively low electron density. However, it is necessary to point out that there is a completely separate explanation which, if verified in later experiments, could lead to a radically different view.

This second interpretation of the events that began at 1134 UT begins by assuming that the density enhancement seen in Figure 9 could be moving downward into the ionosphere. Similarly, the rise in E_w, which was previously assumed to move north to south, could actually have been associated with a downward-moving spatially extended boundary. If this were true one might be tempted to think that the downward-moving density enhancement and subsequent rise of E_w were associated with field-aligned electric fields and anomalous resistivities such that when the density increase reached the upper E region the electron precipitation weakened in intensity and average energy and was finally stopped. At this time the magnetospheric electric field could have penetrated to the lower parts of the ionosphere with its full magnitude.

The second interpretation could lead to an explanation of the previously noted anomaly in Figure 9 where no dramatic increase in electron density could be associated with the passage of the density enhancement through the E region. Such a behavior would be expected if the density enhancement corresponded to some type of plasma accumulation layer rather than a precipitation zone. Likewise, the changes in the E region peak density and altitude might correspond to a weakening of the electron acceleration process.

It must be realized that many aspects of the second interpretation are based upon conjecture. In addition, both the ASC observations of a diffuse band moving in conjunction with the electron density enhancement and the Chatanika zenith observations of 6300 Å argue strongly in favor of the southward-moving wall idea rather than the downward-

moving layer. Nevertheless, the layer interpretation cannot be completely discredited on the basis of the present data, and future experiments will be needed to completely determine the true spatial development.

If we accept the idea that the observed density enhancements were moving southward, the two-dimensional structure (thickness and height) introduces interesting questions about their origin and shape. The radar data indicate that the enhancements extended vertically to about 200 km altitude and that this plasma drifted southward at a fairly uniform speed (see Figure 10). However, it is puzzling that these enhancements do not seem to be simply regions of strong particle precipitation, since as they pass through the 110- to 120-km region there is no apparent proportionate increase in the peak auroral E-region electron density. Thus the main part of the enhancement seems to be in the densities between 130 and 200 km. Such higher densities could be associated with increases in the lower-energy portions of the electron energy spectrum and could perhaps explain why it was difficult to match the ASC auroral results to the southward-moving high-density regions.

The behavior of the intense F_2 layer seen before the 1100 UT substorm onset appears to be anomalous. Yet, for this particular case, the rapid disappearance of the F_2 layer presents a considerable puzzle. If this layer was simply an isolated patch, its disappearance could have been related to horizontal transport associated with the presence of a strong southward electric field at substorm onset; i.e., it moved rapidly southeastward and a new low-density F_2 region moved into the radar line of sight from the northwest. It could also be postulated that vertical motions were involved, moving the excess ionization either upward into the topside ionosphere or downward into the lower ionosphere. However, such motions would involve moving the plasma a distance of at least 100 km within 60 sec, corresponding to parallel speed of 1.6 km sec^{-1} or corresponding line of sight speed of 800 m sec^{-1}. Since such high speeds were not observed, it seems that the peculiar F_2 layer was analogous to a drifting cloud that entered into the radar beam and vanished when the southeastward ion drift speed was suddenly increased.

SUMMARY

In summary, data from the Chatanika incoherent scatter radar have provided a comprehensive view of electric field and plasma variations in the auroral environment. The present experiment confirms the tendency toward reduced values of the westward electric field in regions of higher than average electron density. Secondly, through observations of the electron density enhancements, these regions were seen to drift at approximately the $\mathbf{E}_\perp \times \mathbf{B}$ speed. The plasma inside these enhanced density regions, however, was found to move much more slowly than the surrounding ionization. The thermal structure of these regions did not show any unusual behavior; i.e., the low values of electron temperature are consistent with the electron to ion energy transfer rate which is proportional to n_e^2. Finally, although the present measurements were made during a period of continual magnetospheric disturbance, the variations in the westward electric field appeared to be more strongly linked with local electron density changes than with the overall disturbance pattern deduced from auroral zone magnetograms.

Acknowledgments. The assistance and comments of Drs. J. R. Doupnik, M. Baron, and S.-I. Akasofu are greatly appreciated. The all-sky camera reductions were made by Mr. D. S. Kimball.

This work was supported, in part, through NASA grant NGR-05-009-075 and NSF grant GA-36281 at the University of California, San Diego; NSF grants GA-30351, GA-28042, and GA-32590X at Stanford University; and NSF grant GA-36095 and DNA contract DNA-001-72-C-0076 at Stanford Research Institute.

* * *

The Editor thanks T. N. Davis and J. V. Evans for their assistance in evaluating this paper.

REFERENCES

Aggson, T. L., Probe measurements of electric fields in space, *Atmospheric Emissions*, edited by B. M. McCormac and A. Omholt, p. 305, Van Nostrand Reinhold, New York, 1969.

Axford, W. I., Magnetospheric convection, *Rev. Geophys. Space Phys.*, *7*, 421, 1969.

Banks, P. M., J. R. Doupnik, and S.-I. Akasofu, Electric field observations by incoherent scatter radar in the auroral zone, *J. Geophys. Res.*, *78*, 6607, 1973.

Baron, M. J., DNA project 617 radar: Auroral ionospheric measurements, *Rep. DNA3023F*, Stanford Res. Inst., Menlo Park, Calif., December 1972.

Baron, M. J., O. de la Beaujardiere, and B. Craig, Project 617 radar readiness achievement program, A, Data processing and analysis, *Rep. 2519-1*, Stanford Res. Inst., Menlo Park, Calif., May 1970.

Bates, H. F., A. E. Belon, and R. D. Hunsucker, Aurora and the poleward edge of the main ionospheric trough, *J. Geophys. Res.*, *78*, 648, 1973.

Bering, E. A., M. C. Kelley, and F. S. Mozer, Split Langmuir probe measurements of current density and electric fields in an aurora, *J. Geophys. Res.*, *78*, 2201, 1973.

Brekke, A., J. R. Doupnik, and P. M. Banks, A preliminary study of the neutral wind in the auroral E region, *J. Geophys. Res.*, *78*, 8235, 1973.

Cauffman, D. P., and D. A. Gurnett, Double-probe measurements of convection electric fields with the Injun 5 satellite, *J. Geophys. Res.*, *76*, 6014, 1971.

Chesnut, W. G., J. C. Hodges, and R. L. Leadabrand, Correlation of radar echoes from the aurora with satellite-measured particle precipitation, *Rep. DNA-2825F*, Stanford Res. Inst., Menlo Park, Calif., December 1971.

Choy, L. W., R. L. Arnoldy, W. Potter, P. Kintner, and L. J. Cahill, Field-aligned particle currents near an auroral arc, *J. Geophys. Res.*, *76*, 8279, 1971.

Davis, T. N., Magnetospheric convection pattern inferred from magnetic disturbances and auroral motions, *J. Geophys. Res.*, *76*, 5978, 1971.

Doupnik, J. R., P. M. Banks, M. J. Baron, C. L. Rino, and J. Petriceks, Direct measurements of plasma drift velocities at high magnetic latitudes, *J. Geophys. Res.*, *77*, 4268, 1972.

Evans, J. V., Theory and practice of ionosphere study by Thomson scatter radar, *Proc. IEEE*, *57*, 496, 1969.

Evans, J. V., Ionospheric movements measured by incoherent scatter: A review, *J. Atmos. Terr. Phys.*, *34*, 175, 1972.

Fahleson, U., C. G. Falthammar, A. Pederson, K. Knott, G. Brommundt, G. Schumann, G. Haerendel, and E. Rieger, Simultaneous electric field measurements made in the auroral ionosphere by using three independent techniques, *Radio Sci.*, *6*, 233, 1971.

Föppl, H., G. Haerendel, L. Haser, R. Lüst, F. Melzner, B. Meyer, N. Neuss, H. H. Rabben, E. Rieger, J. Stöcker, and W. Stoffregen, Preliminary results of electric field measurements in the auroral zone, *J. Geophys. Res.*, *73*, 21, 1968.

Galperin, Yu. I., and V. N. Ponomarev, Direct measurements of plasma convection in the upper ionosphere, *Rep. 130*, Acad. of Sci. of the USSR, Inst. for Space Res., Moscow, 1972.

Haerendel, G., Electric fields and their effects in the ionosphere, *Solar Terrestrial Physics*, edited by E. R. Dyer, p. 87, D. Reidel, Dordrecht, Netherlands, 1972.

Haerendel, G., and R. Lüst, Electric fields in the ionosphere and magnetosphere, *Particles and Fields in the Magnetosphere,* edited by B. M. McCormac, p. 213, D. Reidel, Dordrecht, Netherlands, 1970.

Haerendel, G., R. Lüst, E. Rieger, and H. Völk, Highly irregular artificial plasma clouds in the auroral zone, in *Atmospheric Emissions,* edited by B. M. McCormac and A. Omholt, p. 293, Van Nostrand Reinhold, New York, 1969.

Heppner, J. P., Electric fields in the magnetosphere, in *Critical Problems of Magnetospheric Physics,* edited by E. R. Dyer, National Academy of Sciences, Washington, D.C., 1972.

Heppner, J. P., J. D. Stolarik, and E. M. Wescott, Electric-field measurements and the identification of currents causing magnetic disturbances in the polar cap, *J. Geophys. Res., 76,* 6028, 1971.

Kelley, M. C., F. S. Mozer, and U. V. Fahleson, Electric fields in the nighttime and daytime auroral zone, *J. Geophys. Res., 76,* 6054, 1971*a*.

Kelley, M. C., J. A. Starr, and F. S. Mozer, Relationship between magnetospheric electric fields and the motion of auroral forms, *J. Geophys. Res., 76,* 5269, 1971*b*.

Leadabrand, R. L., M. J. Baron, J. Petriceks, and H. F. Bates, Chatanika, Alaska, auroral zone incoherent scatter facility, *Radio Sci., 7,* 747, 1972.

Mozer, F. S., Origin and effects of electric fields during isolated magnetospheric substorms, *J. Geophys. Res., 76,* 7595, 1971.

Mozer, F. S., and P. Bruston, Electric field measurements in the auroral ionosphere, *J. Geophys. Res., 72,* 1109, 1967.

Mozer, F. S., and U. V. Fahleson, Parallel and perpendicular electric fields in an aurora, *Planet. Space Sci., 18,* 1563, 1970.

Mozer, F. S., and R. H. Manka, Magnetospheric electric field properties deduced from simultaneous balloon flights, *J. Geophys. Res., 76,* 1697, 1971.

Mozer, F. S., and R. Serlin, Magnetospheric electric field measurements with balloons, *J. Geophys. Res., 74,* 4739, 1969.

Mozer, F. S., F. H. Bogott, and B. Tsurutani, Relations between ionospheric electric fields and energetic trapped and precipitating electrons, *J. Geophys. Res., 78,* 630, 1973.

Potter, W. E., Rocket measurements of auroral electric and magnetic fields, *J. Geophys. Res., 75,* 5415, 1970.

Potter, W. E., and L. J. Cahill, Electric and magnetic field measurements near an auroral electrojet, *J. Geophys. Res., 74,* 5159, 1969.

Rino, C. L., Radar measurement of ionosphere motion in the presence of current induced spectral asymmetries, *Radio Sci., 7,* 1049, 1972.

Rino, C. L., V. B. Wickwar, P. M. Banks, and S.-I. Akasofu, Incoherent scatter radar observations of westward electric fields, 2, submitted to *J. Geophys. Res.,* 1973.

Subbarao, S., and G. Rostoker, The relationship of southward drifting auroral arcs to the magnetospheric electric field and substorm activity, *J. Geophys. Res., 78,* 1100, 1973.

Watt, T. M., Incoherent scatter observations of the ionosphere over Chatanika, Alaska, *J. Geophys. Res., 78,* 2992, 1973.

Wescott, E. M., J. D. Stolarik, and H. P. Heppner, Electric fields in the vicinity of auroral forms from motions of barium vapor releases, *J. Geophys. Res., 74,* 3469, 1969.

Wescott, E. M., J. D. Stolarik, and J. P. Heppner, Auroral and polar cap electric fields from barium releases, *Particles and Fields in the Magnetosphere,* edited by B. M. McCormac, p. 229, D. Reidel, Dordrecht, Netherlands, 1970.

(Received August 1, 1973;
accepted September 14, 1973.)